On-line Continuous Measurement of the Operating Deflection Shape of Power Transmission Belts Through Electrostatic Charge Sensing

Authors: Yonghui Hu [a]

Yong Yan [b] (Corresponding author)

Lu Yang [a]

Lijuan Wang [b, a]

Xiangchen Qian [a]

Addresses: [a] School of Control and Computer Engineering

North China Electric Power University

Beijing 102206

P. R. China

[b] School of Engineering and Digital Arts

University of Kent

Canterbury

Kent CT2 7NT

UK

Tel: 00441227823015

Fax: 00441227456084

Email: y.yan@kent.ac.uk

ABSTRACT

The measurement of the operating deflection shape (ODS) of power transmission belts is of great importance for the fault diagnosis and prognosis of industrial belt drive systems. This paper presents a novel method based on an electrostatic sensor array to measure the ODS of a belt moving both axially and transversely. The electrostatic sensor integrates a charge amplifier that converts the induced charge on a strip-shaped electrode into a voltage signal. Finite element simulations are performed to study the sensing characteristics of the sensor and the results reveal that the sensor can respond to vibration displacement. Construction of the ODS is achieved in the frequency domain using the ODS frequency response function. Comparative experimental studies with a high-accuracy laser displacement sensor were conducted on a purpose-built test rig and the results show that the vibration frequencies and their relative magnitudes obtained from both sensors agree well with each other. Experiments conducted over a range of belt axial speeds show that the belt vibrates at frequencies that are well separated and identifiable using a peak picking method. The measured ODSs of the first three vibration modes illustrate that the vibration displacement is larger in the middle of the belt span than at both ends and that the phase shift relative to the reference sensor at each measurement point increases monotonically along the belt running direction. The belt axial speed determines the vibration frequencies and displacement, which reaches the maximum amplitude around the natural frequency of the belt.

Index Terms – Belt drive; vibration measurement; electrostatic sensor; charge amplifier; sensor array; operating deflection shape; frequency response function.

I. INTRODUCTION

Belt drives are extensively used to transmit power between shafts in a variety of industrial, automotive, agricultural and home appliance applications. They are frequently preferred to chains

and gears because of simple installation, low maintenance, misalignment tolerance and shock absorption. However, the axially moving belt is prone to vibrations due to the compliance of the material. In addition, a variety of mechanical defects, such as shaft misalignment, pulley eccentricity, belt wear and improper belt tensioning, may give rise to excessive belt vibrations that cause noise radiation, belt fatigue, speed loss and possibly a catastrophic machine failure [1, 2]. In order to monitor the dynamic behaviors of the belt and provide early warning of potential machine failures, it is desirable to measure and characterize the belt vibration on an on-line continuous basis.

A powerful technique for vibration characterization is operating deflection shape (ODS) analysis. An ODS represents the deflection shape a structure exhibits either at a moment in time or at a specific frequency when subjected to dynamic forces. More generally, an ODS can be defined as any forced motion of two or more degrees of freedom on a structure [3, 4]. In contrast with mode shape that characterizes only the resonant vibration of a structure, ODS contains both forced and resonant vibration components. Therefore, ODS analysis enables visualization of the deformation pattern of a structure or machine functioning under normal operating conditions. To construct an ODS, the vibrations at multiple locations of the structure are measured simultaneously. The vibration magnitude and phase of all points define an ODS vector, which can be used for shape animation of the structure. ODS analysis of a power transmission belt is particularly useful in the study of its complex vibration behaviors. The knowledge about the deflection along the length of the belt facilitates the determination of vibration spatial distribution and the troubleshooting of abnormal vibrations without any machine downtime.

In the last few decades, there has been considerable research on the vibration of power transmission belts. However, the majority of studies have focused on dynamic modelling and

theoretical analysis [5, 6], and little research has been undertaken on vibration measurement and ODS analysis, which has been regarded as a challenging task, especially for long-term industrial applications. The axial motion of the belt precludes the employment of conventional contact type sensors such as accelerometers and strain gages. It is also difficult to adapt the various proximity probes developed for the deviation detection of rotating shafts to the measurement of belt vibration. Catalano *et al.* [7] carried out vibration analysis of a belt system using a high-speed camera, which recorded the positions of marked points on the belt. However, the computational overhead of this technique is very high, making it difficult to achieve on-line continuous measurement. Xia *et al.* [8] employed two laser displacement sensors to monitor the vertical and horizontal vibrations of an axially moving string. Agnani *et al.* [9] experimentally investigated the belt vibration behavior using a single-point laser Doppler vibrometer (LDV). Sante and Rossi [10] measured the ODS of a synchronous belt using a scanning LDV for the development of a vibro-acoustic model. Chiariotti *et al.* [11] assessed the dynamic behavior and recovered the ODSs of timing belts in running conditions using a continuous scanning LDV. The laser-based technique can perform non-contact vibration measurement with high sensitivity and high spatial resolution; however, such instruments are prohibitively expensive to implement in routine industrial applications and the use of delicate optical components limits their applicability in dusty, harsh and extreme environments.

In previous studies [12-15], it was found that a dielectric belt running on earthed metal rollers carries electrostatic charge due to contact and frictional electrification. Information about the motion of the belt can be derived using electrostatic sensors placed adjacent to the belt. Specifically, the transverse velocity of the belt can be reflected by the electrostatic signal obtained using a transresistance amplifier (i.e., a current-to-voltage converter) [14, 15]. The electrostatic

sensor is simple, non-contact, inexpensive and suitable for hostile environments, thus representing an appealing solution to the belt vibration measurement problem in industry. The basic concept of belt ODS measurement using an electrostatic sensor array along with preliminary experimental results was first reported in 2016 at the IEEE International Instrumentation and Measurement Technology Conference [15]. This paper presents in detail the fundamental principle, finite element modelling, practical design, implementation and experimental assessment of the measurement system. In particular, the signal from the electrode is conditioned by a charge amplifier instead of the transresistance amplifier used in [15], which permits the characterization of vibration displacement and the construction of the belt ODS from displacement responses.

II. MEASUREMENT PRINCIPLE

A. *Charge-Mode Electrostatic Sensors*

The amount of electrostatic charge accumulated on the belt surface depends on a variety of factors including roller speed, belt material, ambient temperature and humidity. For fixed operating and environmental conditions, the distribution of charge on the belt surface is mainly affected by the surface roughness. Since the non-uniformity of surface roughness is very small, it is reasonable to assume that the charge is evenly distributed on the belt surface. According to the theory of electrostatics, the amount of induced charge on a metal electrode is inversely proportional to the distance between the electrode and the source charge. Therefore, by measuring the induced charge on an electrode located above (or below) the belt, the transverse displacement of the belt can be quantitatively characterized.

In this study, electrostatic sensors working in charge-mode were developed for belt vibration measurement. The essential part of the electrostatic sensor is a charge amplifier that converts the

5

induced charge on the electrode into a voltage signal. Fig. 1 shows a simplified equivalent circuit of the electrode connected to the charge amplifier. The electrode is modelled as a charge source Q_{in} with a shunt capacitor C_{in}. The charge from the electrode is transferred to the range capacitor C_r of an operational amplifier to develop a voltage output V_{out} which can be calculated using the following equation [16]:

$$V_{out} = -\frac{Q_{in}}{C_r}.$$

(1)

Notice that the input capacitance has no effect on the resulting output voltage because the inverting input of the operational amplifier is kept at virtual ground.
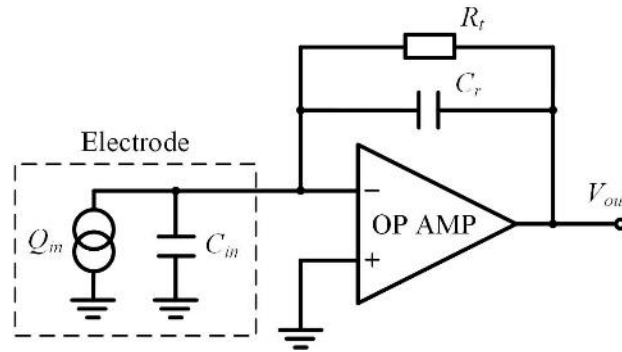
Fig. 1. An equivalent circuit of the electrode connected to a charge amplifier.

In practice, a charge amplifier will drift towards saturation (power supply) due to low insulation resistance at the input or by the leakage current of the input stage of the operational amplifier. Since this study concerns only the AC component of the sensor signal for belt vibration measurement, a time constant resistor R_t is placed in parallel with the range capacitor, as shown in Fig. 1. The accumulated charge on the range capacitor is constantly drained and the DC component of the output voltage goes quickly to zero [16]. The range capacitor and the time constant resistor form a RC-high-pass filter with a lower frequency limit determined by:

$$f_c = \frac{1}{2\pi R_t C_f}.$$

(2)

It is required that the frequency limit is sufficiently lower than the lowest vibration frequency. It is worth noting that an electronic reset switch such as a reed relay or a J-FET placed in parallel with the range capacitor can also be used to periodically bring the output voltage to zero in practical long-term applications [16]. However, the electrode must be taken away or isolated from the electrical field and the induced charge be nulled during reset in order to define the correct zero point, which complicates the design of the sensor unit.

Fig. 2 shows the charge-mode electrostatic sensor manufactured on a compact two-layer printed circuit board (PCB). The electrode is a long pad with a dimension of 3 mm $\times$ 28 mm on the bottom layer. The length of the electrode is identical to the width of the belt to be measured, whereas its width determines the spatial resolution along the belt running direction. The area around the electrode is filled with earthed copper to suppress external electromagnetic interference. On the top layer is the charge amplifier followed by an inverting amplifier and a Salley-Key low-pass filter. The range capacitor of the charge amplifier is a high-quality polystyrene film capacitor with very good performance in terms of dielectric absorption, long-term stability, insulation resistance, *etc*. Since the value of the range capacitor is 10 nF and the voltage gain of the inverting amplifier stage is 50, the sensitivity of the electrostatic sensor is 5 mV/pC. In future practical applications, the inverting amplifier stage can be implemented using a programmable-gain amplifier in order to deal with the variations of charge level on the belt, the distance between the sensor and the belt, and the relative permittivity of the air. The value of the time constant resistor is 1 GΩ, which means the lowest vibration frequency is well above the lower frequency limit (0.016 Hz) of the high-pass filter. In order to guarantee slow drift of the charge measuring circuit, an operational amplifier (Type AD8604) with very low input bias current (typically 0.2 pA) is adopted. A potentiometer at the inverting amplifier stage nulls the

input offset voltage [17]. All components on the top layer are surface-mounted in order to avoid the influence of through-hole pads on the electrical field around the electrode. The sensor unit is powered by a ± 2.5 V dual supply. A standard MINI USB connector is adopted for power and signal transmission because of its compactness, simplicity and reliability.
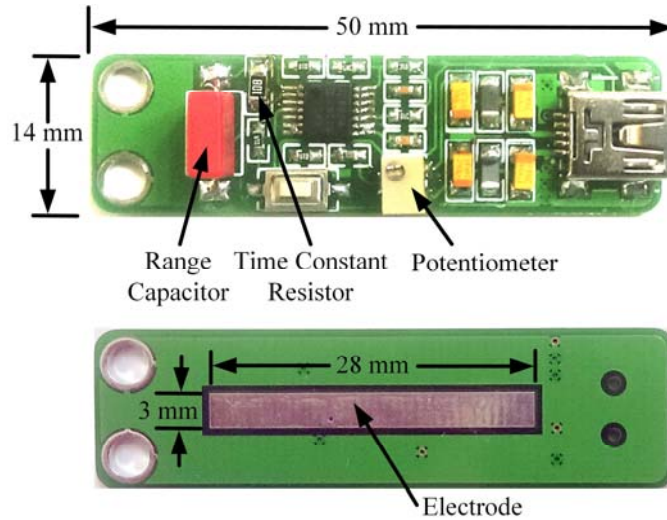

Fig. 2. Charge-mode electrostatic sensor.

B. *Vibration Measurement Through Charge Sensing*

In order to establish a quantitative relationship between the sensor response and belt vibration kinematics, finite element simulations are performed using the commercial software package COMSOL Multiphysics. In view of the superposition principle of the electric field, a point charge that vibrates harmonically in the normal direction of the electrode surface is configured in the modelling. Fig. 3 shows the finite element model finely meshed with tetrahedral elements. The electrode is modelled as a thin copper strip with the same dimension as its physical realization. The point charge is assumed to carry net electrostatic charge of -1 μC. The potential of the electrode is set as zero and the boundary of the model domain is set as zero charge.
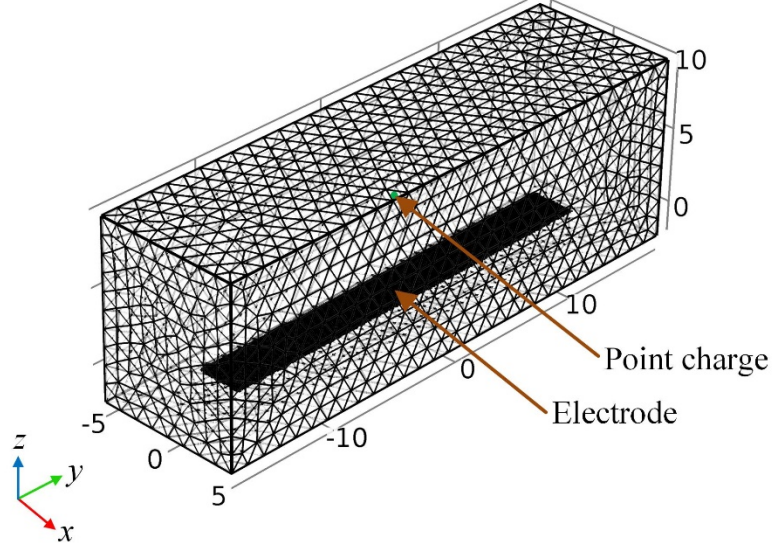
Fig. 3. Finite element model of the electrostatic sensor.

As shown in Fig. 3, the center of the electrode is located at the origin of the coordinate system. The harmonic motion of the point charge is described by

$$z(t) = B + A\sin(2\pi f t) \tag{3}$$

where B represents the equilibrium position, A denotes the vibration amplitude and f is the vibration frequency. Since the charge amplifier responds to the variation of induced charge at the input, the total induced charge on the electrode, which is obtained by integrating the surface charge density, is investigated in this study under different vibration conditions.

Fig. 4 depicts the induced charge for different equilibrium positions and vibration amplitudes for $f = 10$ Hz. As illustrated, the induced charge fluctuates as the point charge approaches and moves away from the electrode reciprocally. For a fixed equilibrium position, a larger vibration amplitude leads to stronger variation of the induced charge. A longer distance between the electrode and the equilibrium position leads to less induced charge and hence a smaller peak-to-peak variation magnitude. It is also noticeable that the fluctuation of the induced charge is unsymmetrical about the value obtained when the point charge is at the equilibrium position, due to the non-uniform spatial sensitivity of the electrostatic sensor [14].
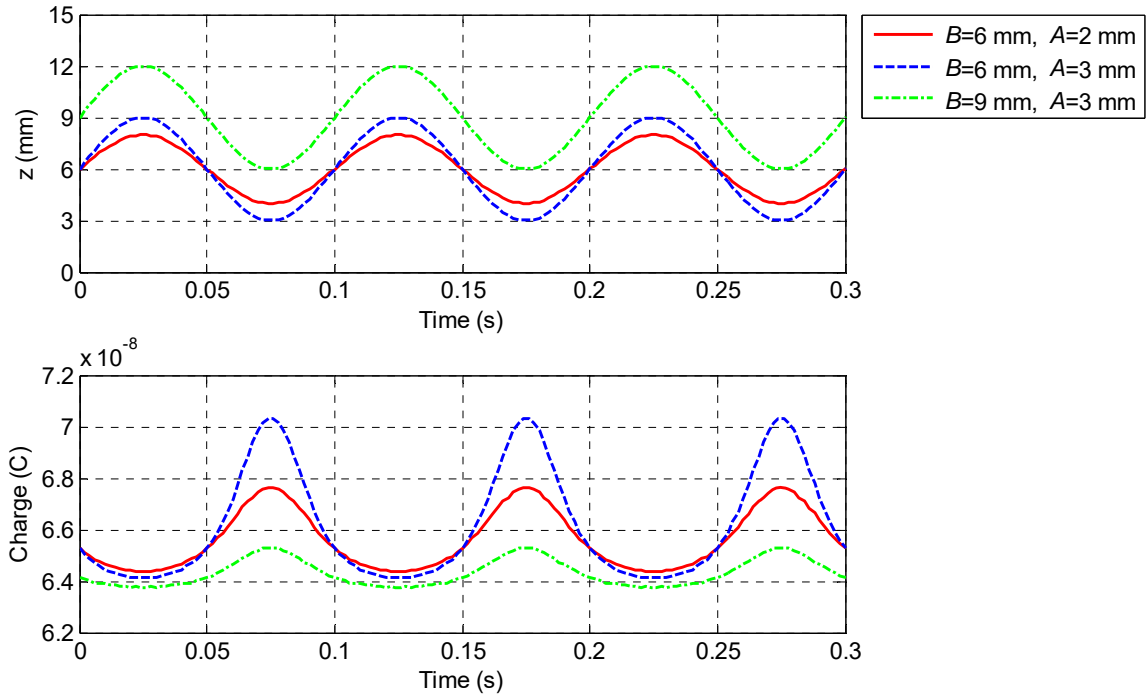
Fig. 4. Induced charge for different equilibrium positions and vibration amplitudes.

The simulation results shown in Fig. 4 suggest that the distance between the electrode and the belt determines the induced charge of the electrostatic sensor. Therefore, it can be used as a non-contact vibration displacement sensor. However, the absolute value of the transverse displacement cannot be measured using the electrostatic sensor due to the vulnerability of the electrostatic sensing technique to environmental and operating conditions. Nevertheless, quantitative characterization of the belt vibration can be achieved using appropriate signal processing techniques.

C. ODS Measurement

Due to the localized sensing zone, the electrostatic sensor measures belt vibration at only a single point. In order to obtain an ODS measurement, multiple sensors arranged in a linear array along the belt length are employed. Fig. 5 illustrates the sensing arrangement of the ODS measurement system.
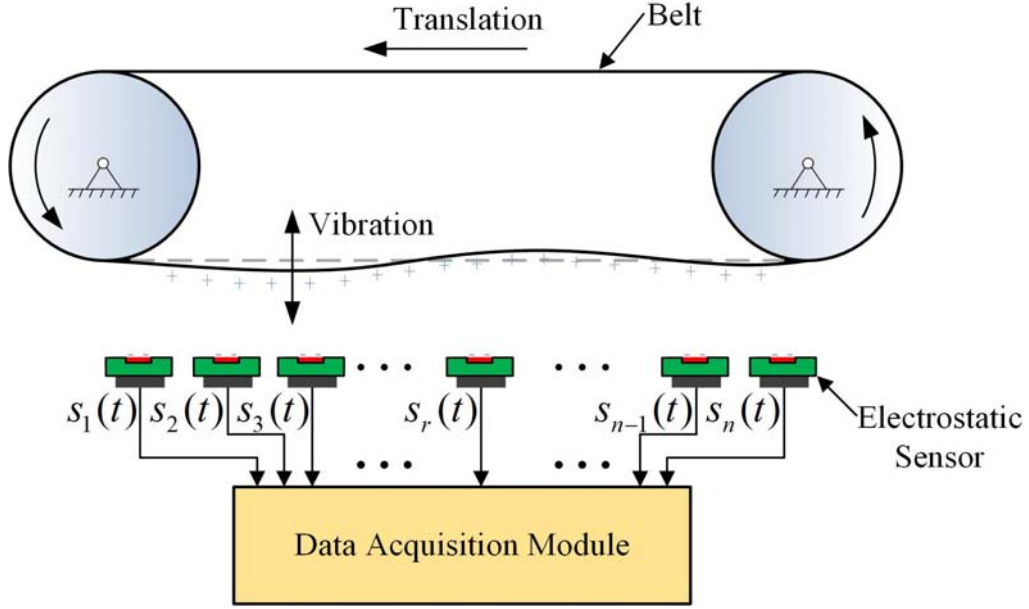
Fig. 5. Sensing arrangement of the measurement system.

An ODS can be derived from a set of time domain signals acquired simultaneously or frequency domain measurements that are computed from the time domain signals [18]. Since the belt exhibits periodic, rather than non-periodic or transient vibration, the ODS frequency response function (FRF) is used to construct the ODS in this study. This technique requires a fixed reference sensor in order to determine the relative phase of each measurement point. To calculate an ODS FRF, the magnitude of the cross spectrum between a sensor signal and the reference sensor signal is replaced with the auto spectrum of the sensor signal. In this way, the correct magnitude of the sensor signal and the correct phase relative to the reference signal are retained. The definition of the ODS FRF is given by the following equation [19]:

$$H_i(\omega) = S_i(\omega)S_i^*(\omega) \bullet \frac{S_i(\omega)S_r^*(\omega)}{|S_i(\omega)S_r^*(\omega)|} \tag{4}$$

where $S_i(\omega)$ and $S_r(\omega)$ represent the Fourier transform of the i-th sensor signal $s_i(t)$ and the reference signal $s_r(t)$, respectively. The operator $*$ denotes the complex conjugate. The first term

in equation (4) represents the auto spectrum of the i-th sensor signal and the second term the phase of the cross spectrum between the i-th sensor signal and the reference signal. In comparison with other frequency domain functions such as linear spectra, auto power spectra, FRFs and transmissibility [18], the ODS FRF provides an absolute measurement instead of a ratio of the magnitude responses, contains the correct phase relative to the reference and allows easy identification of the peak frequencies.

For a variety of belt operation issues such as eccentricity, misalignment, worn and stretched belts, the vibrations occur at the belt pass frequency and its higher-order harmonics, which are well-separated and can be identified using the so-called peak-picking method [20]. Since the response of the electrostatic sensor working in charge-mode represents the transverse displacement, the imaginary components of the ODS FRFs at vibration frequency ω_k are assembly as follows to yield the k-th ODS vector φ_k [20, 21]:

$$\varphi_k = \begin{Bmatrix} \mathrm{Im}[H_1(\omega_k)] \\ \mathrm{Im}[H_2(\omega_k)] \\ \vdots \\ \mathrm{Im}[H_r(\omega_k)] \\ \vdots \\ \mathrm{Im}[H_n(\omega_k)] \end{Bmatrix} \tag{5}$$

where n is the number of sensors deployed, with one of them being the reference sensor.

III. EXPERIMENTAL RESULTS AND DISCUSSION

A. Experimental Setup

Experiments with the measurement system were conducted on a purpose-built test rig, as shown in Fig. 6. The rig consists of a flat nylon-type belt and two earthed metal pulleys with an

equal diameter. The running speed of the belt can be adjusted by regulating the rotational speed of a driving motor. A total of 20 electrostatic sensors with an equal spacing of 20 mm between adjacent elements are supported by a lab stand above the belt. Since the center-to-center distance between the two pulleys is 390 mm, the sensor array covers almost the whole slack side of the belt span. A closer spacing between the sensor and the belt helps improve the signal-to-noise ratio but also increases the risk of direct contact between them and hence the potential damage of the sensor by the belt. In this study, the spacing from the sensor array to the belt in stationary state is set as 15 mm by taking into consideration the maximum transverse displacement of the belt. A power board generates ± 2.5 V supplies for the sensor units and receives the analog sensor outputs.
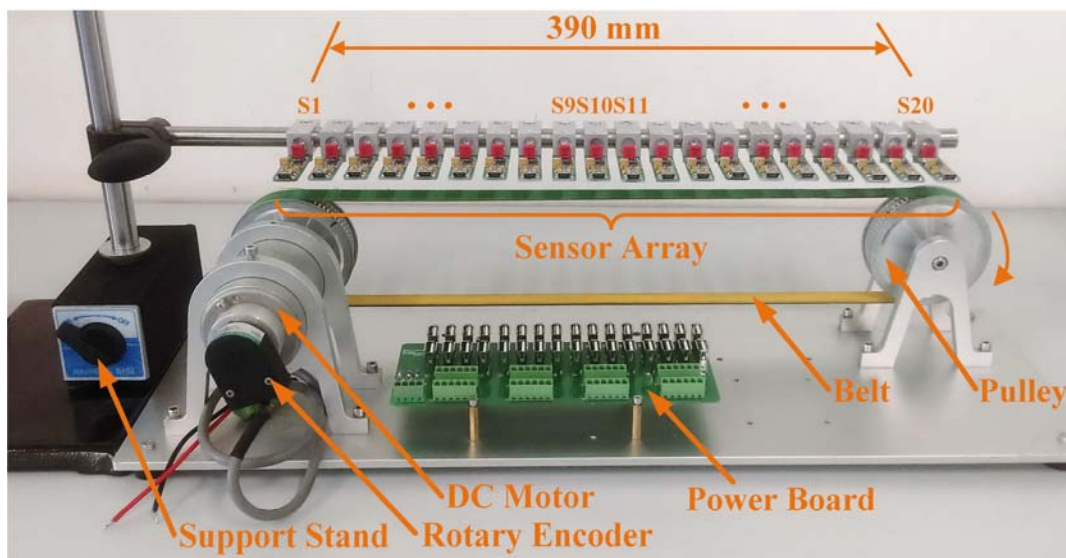
Fig. 6. Motor driven belt rig.

The sensor signals were sampled simultaneously at a frequency of 50 kHz using a data acquisition (DAQ) device (National Instruments, model USB-6363) and processed on a host computer. In order to achieve on-line ODS measurement, a dedicated software system was developed using Microsoft Visual C# .NET with the aid of National Instruments Measurement Studio, which provides class libraries for communication with NI DAQ devices, data processing

and storage, user interface design, and data visualization. In comparison with the graphical programming language LabVIEW, it is more convenient to implement complex algorithms such as peak-picking and ODS measurement using the text-based programming language Visual C#. Since the computational overhead of the ODS measurement algorithm is low, the measurement results can be delivered almost in real time for each acquisition time interval, thus exhibiting advantages over the imaging-based off-line method in [7].

B. Vibration Measurement Results

Before the measurement of the belt ODS, the performance of the electrostatic sensor for vibration measurement was validated against a laser displacement sensor (Controller model LK-G5001 and sensor head model LK-H085, Keyence CO., Ltd.) that measures its distance to the belt with high accuracy. Fig. 7 shows the installation of the electrostatic and laser displacement sensors on the test rig. Due to the obstruction of the laser light by the electrostatic sensor plate, the measurement point of the laser displacement sensor doesn't coincide with the point on the belt right underneath the center of the electrode, leaving a gap of about 8 mm between them, as shown in Fig. 7. The analog outputs of both sensors were sampled simultaneously using the NI DAQ device.
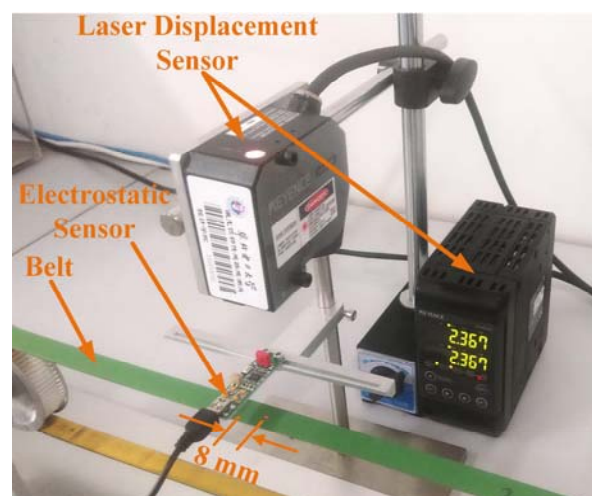

Fig. 7. Installation of the electrostatic and laser displacement sensors on the test rig.

Fig. 8 shows the measurements from both sensors when the belt axial speed is 5.3 m/s. Note that the voltage signal of the laser displacement sensor has been converted proportionally into transverse displacement. It is shown that the belt vibrates with a peak-to-peak displacement of 0.9 mm. Clear periodicity and similar patterns are observed in both measurements. The time delay between the measurements is attributed to the gap between the measurement points. In order to quantify the similarity, cross-correlation analysis is performed, with each measurement normalized with respect to its peak amplitude [13]. A correlation coefficient of 0.6 is obtained, suggesting that the two measurements are strongly correlated. In addition, the frequency spectra of the measurements are plotted in Fig. 9, in which normalization is also performed separately with respect to the highest spectral peaks. It is evident that there exist strong, well-separated spectral peaks in both measurements. These vibration frequencies satisfy an integer multiple relationship with the fundamental frequency. With reference to the laser displacement sensor, the electrostatic sensor can identify the vibration frequencies accurately. The relative magnitudes of the spectral peaks in both measurements are in good agreement, with slight difference especially for the first two harmonics due to the different sensing mechanisms.
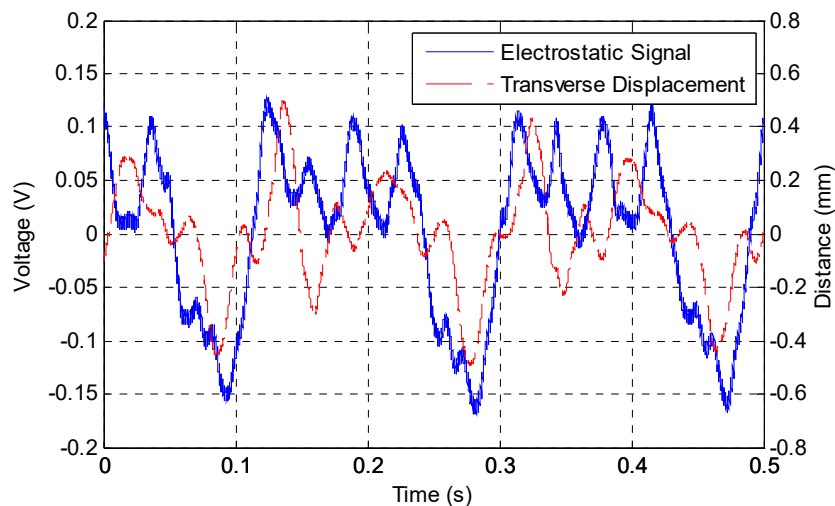

Fig. 8. Measurements from the electrostatic and laser displacement sensors when the belt axial speed is 5.3 m/s.
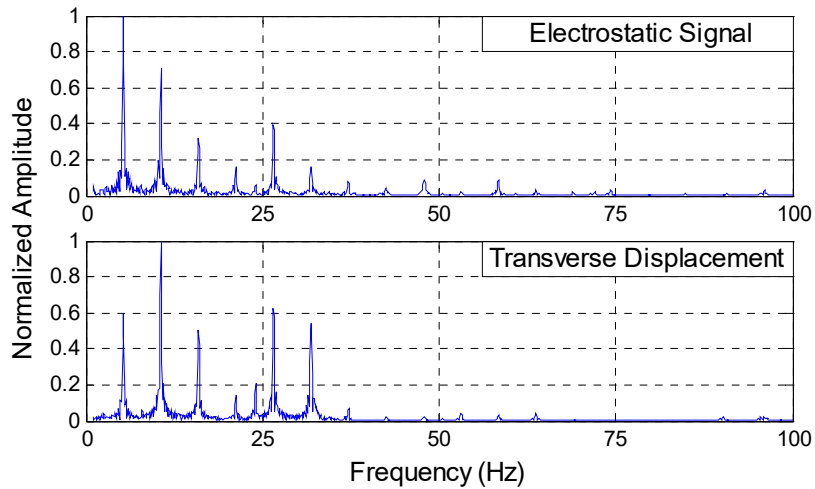
Fig. 9. Normalized amplitude spectra of the electrostatic and laser displacement measurements.

As has been pointed out above, the amount of electrostatic charge deposited on the belt depends on a variety of environmental conditions, among which the humidity is considered to have a strong impact and thus investigated in this study [22]. An ultrasonic humidifier was used to emit water vapor into the air. The relative humidity was varied from 55% to 95%, while the temperature was held constant at 22 ºC and the belt axial speed at 6.0 m/s. The experimental results illustrate that the electrostatic sensor can identify the vibration modes and their relative magnitudes over the whole range of humidity conditions tested. To quantify the effect of humidity on the strength of the electrostatic signal, the RMS (root-mean-square) magnitude of the electrostatic signal was calculated and shown in Fig. 10. It illustrates that the RMS magnitude decreases with the humidity, suggesting that less charge is accumulated on the belt. Therefore, in order to ensure the operability of the sensing unit in a humid environment, the electrostatic signal should be adequately amplified. In view of the susceptibility of the charge level on the belt to environmental conditions in real-world applications, a signal conditioning circuit with programmable gain can be employed to convert the induced charge into a voltage signal at a suitable level for subsequent A/D conversion.
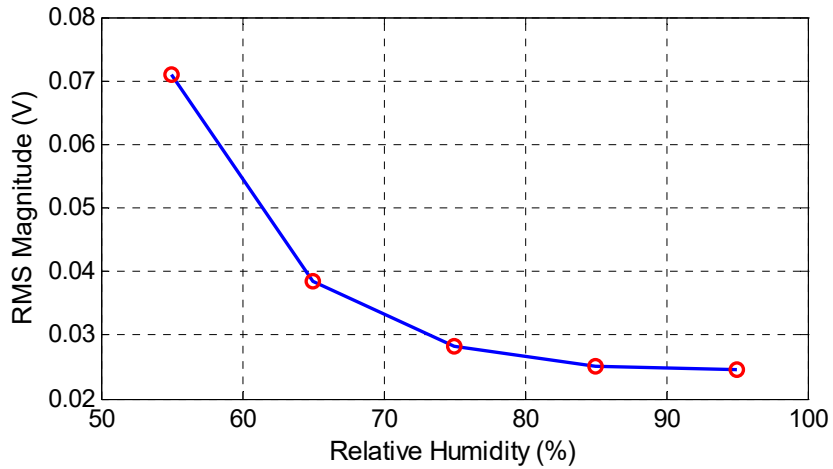
16

Fig. 10. RMS magnitude of the electrostatic signal as the relative humidity of air varies.

C. ODS Measurement Results

After the validation of the effectiveness of the technique for belt vibration measurement, the electrostatic signals from the sensor array were collected. Fig. 11 shows five typical electrostatic signals from sensors S1, S9, S10, S11 and S20, as labelled in Fig. 6, when the belt axial speed is 6 m/s. The signals from the sensors S9, S10 and S11, which are located above the center of the belt span, exhibit clear periodicity. It is also evident that a downstream signal is a time-delayed, but corrupted version of its preceding one. If the belt vibration can be regarded as a travelling wave that propagates along the belt length, the sensors in the array experience different phases of the travelling wave, leading to the phase shifts between the signals. Sensors S1 and S20 located close to the pulley generate signals with smaller vibration amplitude, because of the decreased vibration displacement.
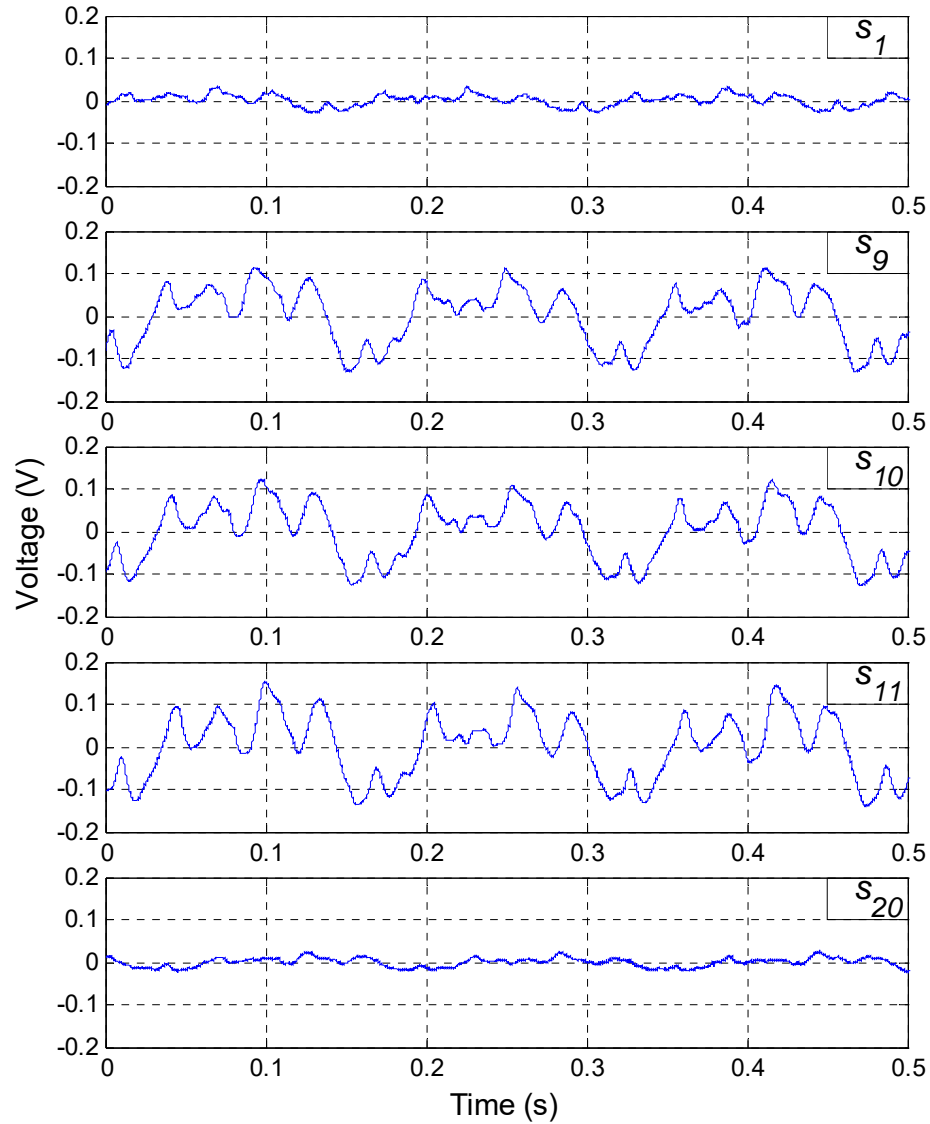
17

Fig. 11. Signals from sensors S1, S9, S10, S11 and S20 at a belt axial speed of 6 m/s.

The amplitude spectra of the electrostatic signals in Fig. 11, but of a longer period of time (2 s), are plotted in Fig. 12, which illustrates that the vibrations occur at the same frequencies along the belt span. It is also noticeable that the signals share almost the same relative magnitudes of the spectral peaks. In comparison with the velocity response measured using electrostatic sensors with transresistance amplifiers [15], there are fewer spectral peaks at higher frequencies and the fundamental vibration mode has the largest magnitude. Note that the small spectral peaks at 50 Hz in Fig. 12 are due to the power line noise.
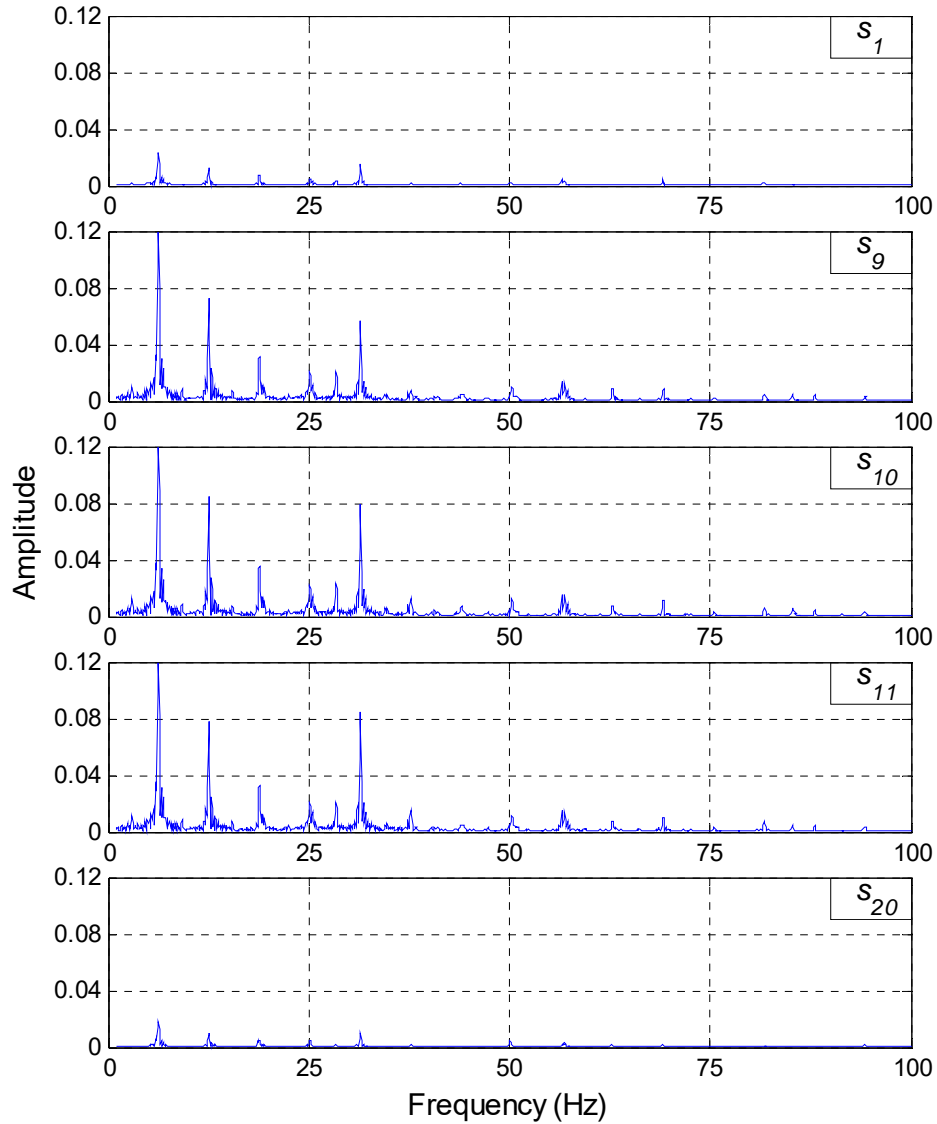
Fig. 12. Amplitude spectra of the electrostatic signals in Fig.11.

To calculate the ODS FRFs of the belt, sensor S1 with the least vibration is selected as the reference. According to equation (5), the imaginary components of the complex-valued ODS FRFs at the lower frequency band (0 to 40 Hz) are plotted in Fig. 13. As illustrated, the peaks in the amplitude spectra appear at the same frequencies in the ODS FRFs. Hence the method of peak picking can be used to identify the vibration frequencies. By connecting the peaks at the same frequency in Fig. 13, the belt ODSs can be constructed. Fig. 14 depicts the ODSs corresponding to the first three vibration modes. It can be seen that the three ODSs exhibit similar deformation

patterns, apart from the differences in amplitude. Since an ODS contains both amplitude and phase information, Fig. 15 plots the vibration amplitude and the phase relative to the fixed reference sensor for the first vibration mode at each measurement point. As can be seen in Fig. 15(a), the vibration amplitude is smallest at both ends and slightly decreases in the middle of the belt span. Fig. 15(b) shows that the phase lag increases monotonically along the belt running direction. In view of the above information, it should be noted that the choice of the reference sensor affects the bending shape of an ODS.
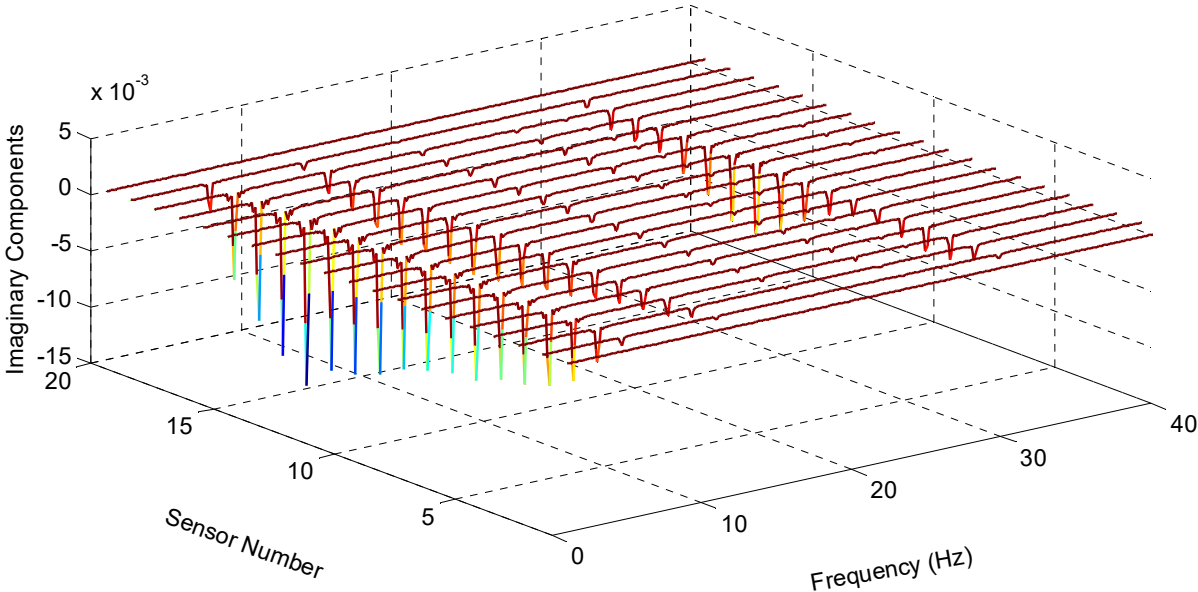
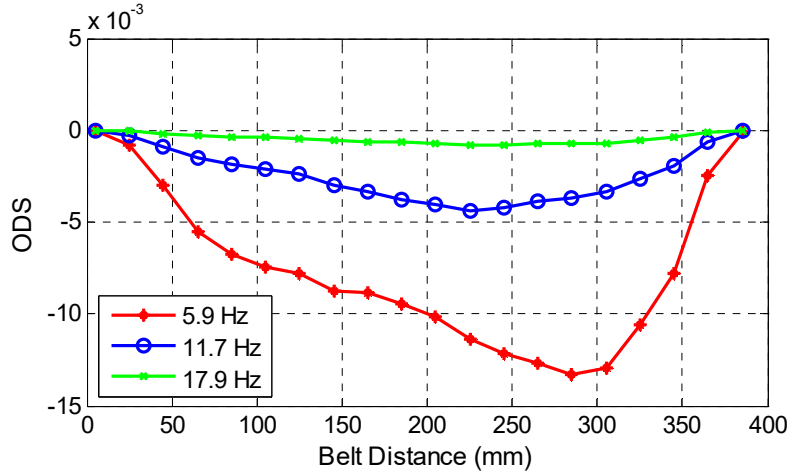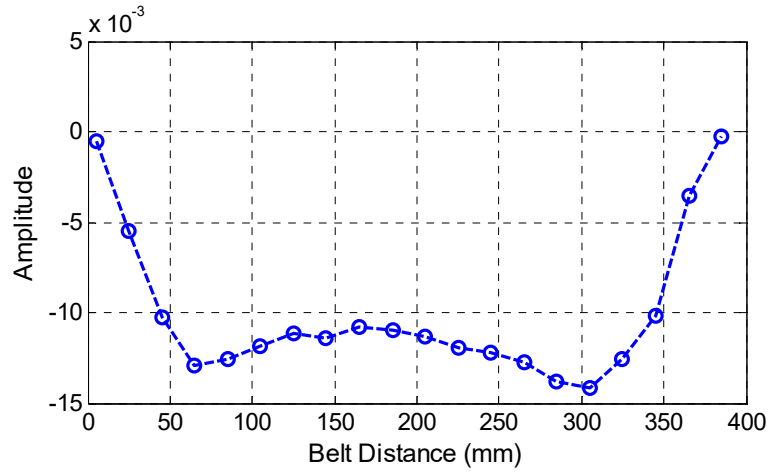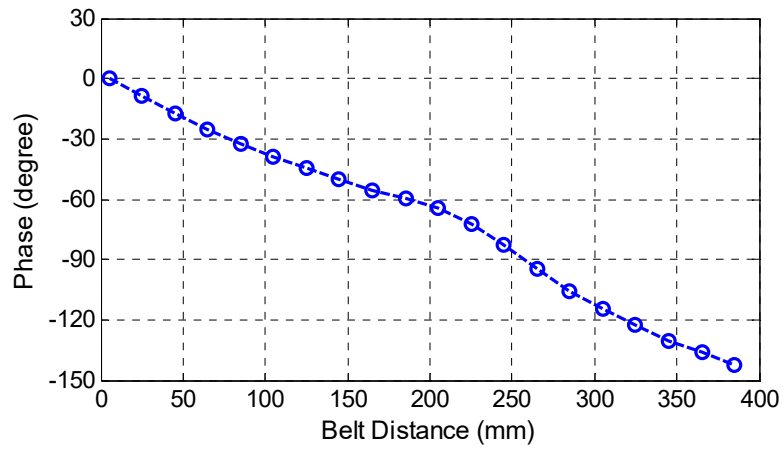Fig. 13. Imaginary components of the ODS FRFs.

Fig. 14. The first three ODSs.

(a) Vibration amplitude along the belt span.

(b) Phase relative to the reference.

Fig. 15. Vibration amplitude and phase relative to the reference for the first ODS.

The ODSs at different belt axial speeds are plotted in Fig. 16. As labelled in the legends, the vibration frequencies increase with the belt axial speed. The bending shape of the ODSs at different axial speeds are very alike. The ODS amplitudes increase with the belt axial speed from 2 m/s to 6 m/s (shown in Fig. 14), but exhibit a decreasing trend from 8 m/s to 10 m/s. According to the theory of mechanical vibration, the maximum amplitude of vibration occurs when the forcing frequency coincides with a system's natural frequency. It is therefore believed that the belt's natural frequency is around 6 Hz to 8 Hz.
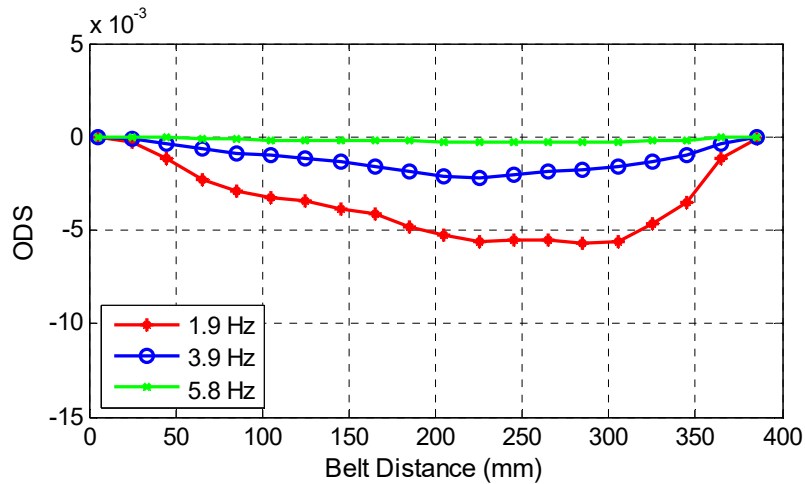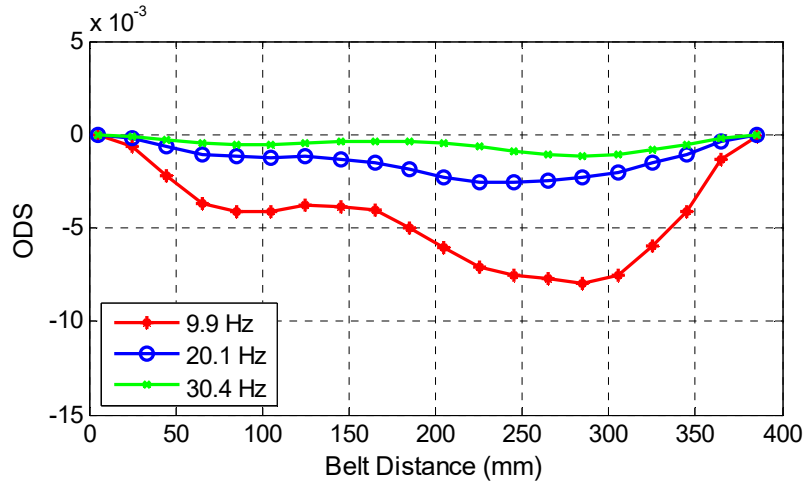

(a) 2 m/s.
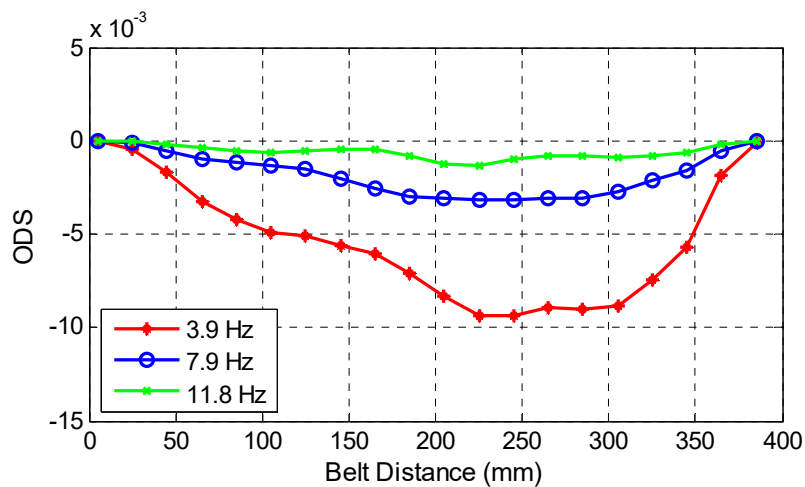
(b) 4 m/s.
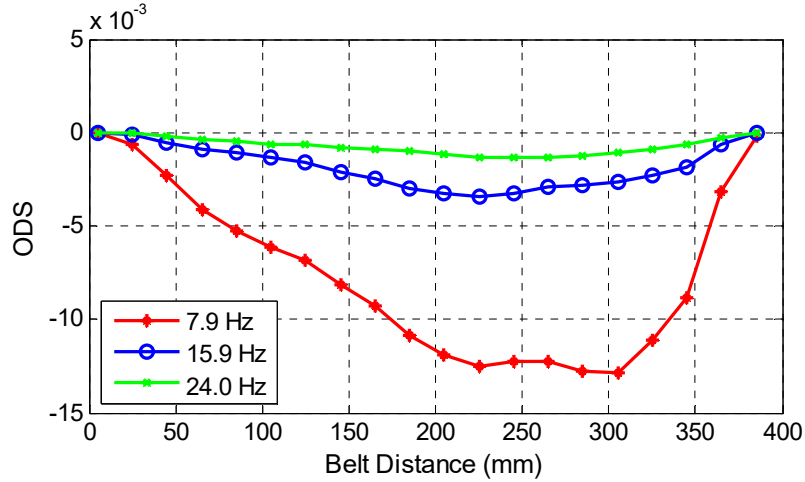
(c) 8 m/s.

(d) 10 m/s.

Fig. 16. Measured ODSs at different axial speeds.

D. Discussion

In comparison with the laser-based instruments that are accurate, expensive, complex and delicate, the electrostatic sensor is cost-effective, compact in size, simple in structure, easy to install and rugged for use in a hostile environment. However, it is difficult to achieve absolute displacement measurement using the electrostatic sensor due to the uncertain amount of charge on the belt. In most condition monitoring applications, the vibration frequency rather than the displacement provides the most valuable information. The electrostatic sensor can identify the

vibration modes and their relative magnitudes with adequate accuracy, thus offering a viable solution to the belt vibration monitoring problem.

The electrostatic sensor is vulnerable to electromagnetic interference due to the working principle of electrostatic induction. In an industrial environment with various electrical machines and devices, the interference may be strong enough to disrupt the normal operation of the sensor. Shielding of the sensing units and the belt with an earthed metal screen is required when working in a complex electromagnetic environment. The installation of the sensor array and the metal screen requires the area of the whole belt span to be cleared. It is thus recommended that ample space is made available for such installation at the design phase of the belt-driven equipment.

Industrial belts may experience resonance and vibrate excessively, which leads to electrostatic signals with high peak-to-peak amplitudes. Corrective and preventive actions such as automated system shutdown should be taken immediately when excessive belt vibrations are detected. In addition to possible damage to the machine, excessive belt vibrations may cause direct contact between the sensor and the belt. In the interest of safety, the spacing between the sensor and the belt should be large enough. However, the signal-to-noise ratio will deteriorate as the induced charge on the electrode decreases with the spacing. Therefore, the maximum transverse displacement of the belt should be estimated for adequate installation of the sensor. A dielectric plate placed between the sensor and the belt can also be used for protection.

Normally, the outside surfaces of flat belts, multi-groove belts and synchronous belts are smooth or have uniform textures. The assumptions of uniform roughness and charge distribution over the belt hold well for such belts. However, the charge distribution is non-uniform when the belt is worn. An abrupt change in the signal amplitude is expected when the worn part passes the sensor unit. The health condition of the belt can thus be evaluated through the analysis of the non-

stationary electrostatic signal. In practice, a worn belt may lead to abnormal vibrations, which can also be used to indicate an incipient machine failure.

The charge-mode electrostatic sensor generates an AC voltage signal that varies inversely with the spacing between the electrode and the object to be measured. By contrast, the electrostatic sensor with a transresistance amplifier responds to the variation rate of induced charge and delivers velocity response [13-15]. A plot of the velocity spectrum will slope upwards as the frequency increases in comparison with the displacement spectrum for the same vibration. The choice of displacement or velocity measurement can be made according to the different frequency ranges of interest.

To summarize, in view of the fact that the techniques available for non-contact vibration measurement of power transmission belts are very limited, the electrostatic sensor provides a promising solution for widespread, routine industrial applications.

IV. CONCLUSION

In this paper, a novel measurement system based on an array of charge-mode electrostatic sensors has been designed and implemented to measure the ODS of a power transmission belt. Finite element simulations have been conducted to establish the relationship between the sensor response and the belt vibration kinematics. ODS FRFs have been used to construct the belt ODS at the fundamental and higher-order harmonic vibration frequencies. The performance of the measurement system has been assessed with reference to the laser displacement sensor. Results obtained have demonstrated that the belt vibrates at frequencies determined by belt axial speed, which permits the construction of the ODS using the peak picking method. The effect of humidity on the performance of the electrostatic sensor has also been experimentally investigated. Although

the RMS magnitude of the electrostatic signal decreases with the humidity due to reduced charge level on the belt, the vibration modes and their relative magnitudes can be identified with adequate accuracy. The measured ODSs of the first three vibration modes exhibit similar bending shapes. The belt ODSs at different axial speeds have indicated that the vibration displacement varies with the axial speed and reaches the maximum amplitude around the belt's natural frequency.

ACKNOWLEDGMENT

REFERENCES

[1] J. Moon, J. A. Wickert, "Non-linear vibration of power transmission belts," *Journal of Sound and Vibration*, vol. 200, no. 4, pp. 419-431, 1997.

[2] N. V. Gaiko, W. T. van Horssen, "On the transverse, low frequency vibrations of a traveling string with boundary damping," *Journal of Vibration and Acoustics - Transactions of the ASME*, vol. 137, no. 4, p. 041004, 2015.

[3] B. J. Schwarz and M. H. Richardson, "Introduction to operating deflection shapes," *CSI Reliability Week*, Orlando, Florida, October 1999.

[4]   B. Weekes and D. Ewins, "Multi-frequency, 3D ODS measurement by continuous scan laser Doppler vibrometry," *Mechanical Systems and Signal Processing*, vol. 58-59, pp. 325-339, 2015.

[5]   L. Q. Chen, "Analysis and control of transverse vibrations of axially moving strings," *Applied Mechanics Reviews*, vol. 58, no. 2, pp. 91-116, 2005.

[6]   K. Marynowski and T. Kapitaniak, "Dynamics of axially moving continua," *International Journal of Mechanical Sciences*, vol. 81, pp. 26-41, 2014.

[7]   P. Catalano, F. Fucci, F. Giametta, G. L. Fianza and B. Bianchi, "Vibration analysis using a contactless acquisition system," *Proceedings of SPIE*, vol. 8881, 888108, 2013.

[8]   C. Xia, Y. Wu and Q. Lu, "Experimental study of the nonlinear characteristics of an axially moving string," *Journal of Vibration and Control*, vol. 21, no. 16, pp. 3239-3253, 2014.

[9]   A. Agnani, M. Martarelli and E. P. Tomasini, "V-belt transverse vibration measurement by means of laser Doppler vibrometry," *Proceedings of SPIE*, vol.7098, 709819, 2008.

[10] R. D. Sante and G. L. Rossi, "A new approach to the measurement of transverse vibration and acoustic radiation of automotive belts using laser Doppler vibrometry and acoustic intensity techniques," *Measurement Science and Technology*, vol. 12, no. 4, pp. 525–533, 2001.

[11] P. Chiariotti, M. Martarelli, P. Castellini, "Exploiting continuous scanning laser Doppler vibrometry in timing belt dynamic characterisation," *Mechanical Systems and Signal Processing*, in press, available online 21 January 2016.

[12] Y. Yan, S. J. Rodrigues and Z. Xie, "Non-contact strip speed measurement using electrostatic sensing and correlation signal-processing techniques," *Measurement Science and Technology*, vol. 22, no. 7, 075103, 2011.

[13] Y. Hu, Y. Yan, L. Wang, X. Qian and X. Wang, "Simultaneous measurement of belt speed and vibration through electrostatic sensing and data fusion," *IEEE Transactions on Instrumentation and Measurement*, vol. 65, no. 5, pp. 1130-1138, 2016.

[14] Y. Hu, Y. Yan, L. Wang and X. Qian, "Non-contact vibration monitoring of power transmission belts through electrostatic sensing," *IEEE Sensors Journal*, vol. 16, no. 10, pp. 3541-3550, 2016.

[15] Y. Hu, L. Yang, L. Wang, X. Qian and Y. Yan, "On-line continuous measurement of the operating deflection shape of power transmission belts through electrostatic sensing," in *Proceedings of IEEE International Instrumentation and Measurement Technology Conference*, pp. 872–876, Taipei, China, May 2016.

[16] G. Gautschi, *Piezoelectric Sensorics: Force, Strain, Pressure, Acceleration and Acoustic Emission Sensors, Materials and Amplifiers*, Germany: Springer-Verlag Berlin Heidelberg, 2002.

[17] S. Franco, *Design with Operational Amplifiers and Analog Integrated Circuits*, 4th edition. McGraw-Hill Education, 2014.

[18] P. L. McHargue and M. H. Richardson, "Operating deflection shapes from time versus frequency domain measurements," in *Proceedings of the 11th International Modal Analysis Conference*, Kissimmee, Florida, USA, February 1-4, 1993.

[19] W. Bae, Y. Kyong, J. Dayou, K. Park and S. Wang, "Scaling the operating deflection shapes obtained from scanning laser Doppler vibrometer," *Journal of Nondestructive Evaluation*, vol. 30, no. 2, pp. 91-98, 2011.

[20] J. P. Lynch, Y. Wang, K. J. Loh, J. Yi and C. Yun, "Performance monitoring of the Geumdang Bridge using a dense network of high-resolution wireless sensors," *Smart Materials and Structures*, vol. 15, no. 6, pp. 1561-1575, 2006.

[21] M. H. Richardson, "Modal analysis using digital test systems," Seminar on Understanding Digital Control and Analysis in Vibration Test Systems, Shock and Vibration Information Center Publication, Naval Research Laboratory, Washington D.C., May 1975.

[22] S. H. S. Javadi and D. H. Napier, "Electrification of dielectric belts running on earthed metal rollers," *IChemE Symposium Series*, no. 39a, pp. 266-279, 1974.